GEOLOGICA BELGICA
2022, Vol. 25/1-2, 17–30
https://doi.org/10.20341/gb.2021.008

Frasnian reef mounds in the Durbuy–Bomal area (eastern border of the Dinant Synclinorium, Belgium)

FRÉDÉRIC BOULVAIN

Pétrologie sédimentaire, B20, Quartier Agora, Université de Liège, Sart Tilman, B-4000 Liège, Belgium; ***corresponding author****: fboulvain@uliege.be.*

NICOLAS DEMAUDE

Pétrologie sédimentaire, B20, Quartier Agora, Université de Liège, Sart Tilman, B-4000 Liège, Belgium.

FANNY TOUSSAINT

Pétrologie sédimentaire, B20, Quartier Agora, Université de Liège, Sart Tilman, B-4000 Liège, Belgium.

MARIE COEN-AUBERT

DO Terre & Histoire de la Vie (Evolution de la Paléobiosphère), Institut royal des Sciences naturelles de Belgique, rue Vautier 29, B-1000 Bruxelles, Belgium; mcoenaubert@naturalsciences.be.

ABSTRACT

This paper focuses on the Frasnian reefal development in the eastern border of the Dinant Synclinorium. Classical sections from the Durbuy–Bomal area were reevaluated for lithostratigraphy, microfacies, magnetic susceptibility (MS) and diagenesis. As regards the middle Frasnian succession, the studied area is located in a transitional zone between the Pont de la Folle/Philippeville Formations and the Moulin Liénaux/Grand Breux Formations. This succession is topped by Petit-Mont Member reef mounds. Massive mound microfacies are characteristic of the Petit-Mont and Lion Members, with fossil associations respectively dominated (from deepest to shallowest) by sponges; sponges, crinoids and corals; corals, crinoids, stromatoporoids and cyanobacteria; and microbes. Flank and off-mound microfacies consist of microbioclastic, bioclastic, crinoidal or lithoclastic bedded limestones. MS values are related to the depositional environment and regularly decrease from the off-mound to the reef mound microfacies. The reef mound diagenetic sequence is similar to that identified in other Petit-Mont buildups: cementation in the marine phreatic zone preliminary to drowning, then the development of a meteoric lens at the time of a marine regression, with dysoxic facies in the distal zones of the aquifer and, finally burial cementation and dolomitization during the Variscan tectonism.

KEYWORDS

reef mound,
microfacies,
lithostratigraphy,
magnetic susceptibility,
diagenesis,
palaeogeography

Article history

Received 06.12.2019, accepted in revised form 22.12.2021, available online 20.04.2022.

1. Introduction

In Wallonia (Belgium), Frasnian formations are noteworthy for their high degree of lateral variation. Most of the studies focused on an N-S transect, corresponding to a proximal-distal evolution (Boulvain et al., 1999; Fig. 1). With the significant exception of studies by de Magnée (1930, 1932) and Coen (1973, 1974), the eastern border of the Dinant Synclinorium deserved relatively little interest. This study aims to document the reef mound development in the Durbuy and Bomal areas.

From a structural point of view, the Durbuy area is characterised by a series of SW-NE trending anticlines and synclines affected by longitudinal faults (Fourmarier, 1900; 1931) (Fig. 2). Bellière (1954), after de Magnée (1932), highlighted a difference in tectonic style between the Durbuy anticline tentatively coupled to the northwestern Philippeville area and the border of the Dinant Synclinorium itself. In the Durbuy area indeed, most folds are upright and relatively symmetrical, with 50–60° NW or SE dipping limbs, but some folds are inclined, with a SE vergence and are associated with NW dipping faults like in the Philippeville area (e.g. Sacré, 1943; Fourmarier, 1954; Dumoulin & Marion, 1997a, 1997b; Barchy & Marion, 2008). Southeasterly, the fold wavelength

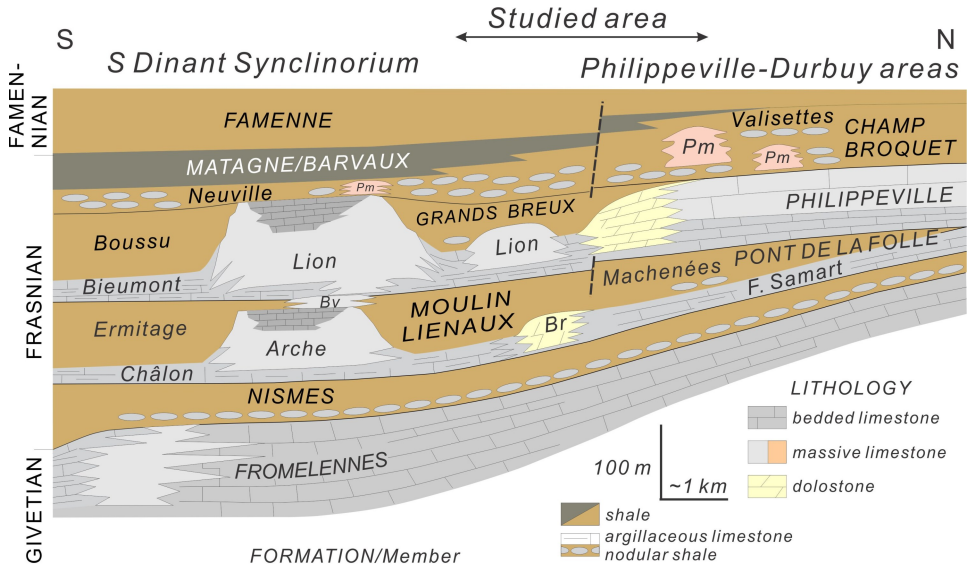

Figure 1. Cross section in the southern part of the Dinant Synclinorium before the Variscan structuration. Pm: Petit-Mont Member; Br: Brayelles Member; Bv: Boverie Member; F. Samart: Fontaine Samart Member.

decreases and folds are overturned, with 70–80°SE and 50°SE dipping limbs (north vergence). Fold axes plunge shallowly to the southwest. Except for the Bomal Fault which is a strike-slip fault, faults are reverse faults mainly located on the NW limbs of anticlines and displaying steep dips to the SE.

Stratigraphically, during the middle Frasnian, the studied area is located in a transitional zone between the Pont de la Folle/Philippeville Formations (also observed in the northwestern part of the Philippeville area) and the Moulin Liénaux/Grand Breux Formations (cropping out in the SE of the Philippeville area and the southern border of the Dinant Synclinorium; Dumoulin et al., 1998; Boulvain et al., 1999; Barchy & Marion, 2008) (Fig. 1). The shaly upper part of the Frasnian corresponds to the Neuville and Les Valisettes Members of the Champ Broquet Formation (Coen-Aubert, 2015, 2016) and to the Barvaux Formation (Figs 1 & 2). Well-developed reef mounds from the Petit-Mont Member are observed around Durbuy (de Magnée, 1932), the most spectacular being the Rome buildup (Dumon, 1982), currently included in a leisure park.

Four sections were studied and sampled in the Durbuy area: Rocher Glawan, Roche Plissée, Ravin d'Herbet and Rome mound (Table 1). The first section is located north of the Herbet Fault whereas the other three are situated between the Herbet and Bomal Faults (Fig. 2).

2. Methods

Petrographic samples for thin sections (490 for the present study) were selected from all facies, even unconsolidated. In that case, samples were indurated with Geofix® resin. Cathodoluminescence observations were made on a CITL Mk5 -2 device (11 kV and 250 µA). All the thin sections are kept at the Laboratoire de Pétrologie sédimentaire of the University of

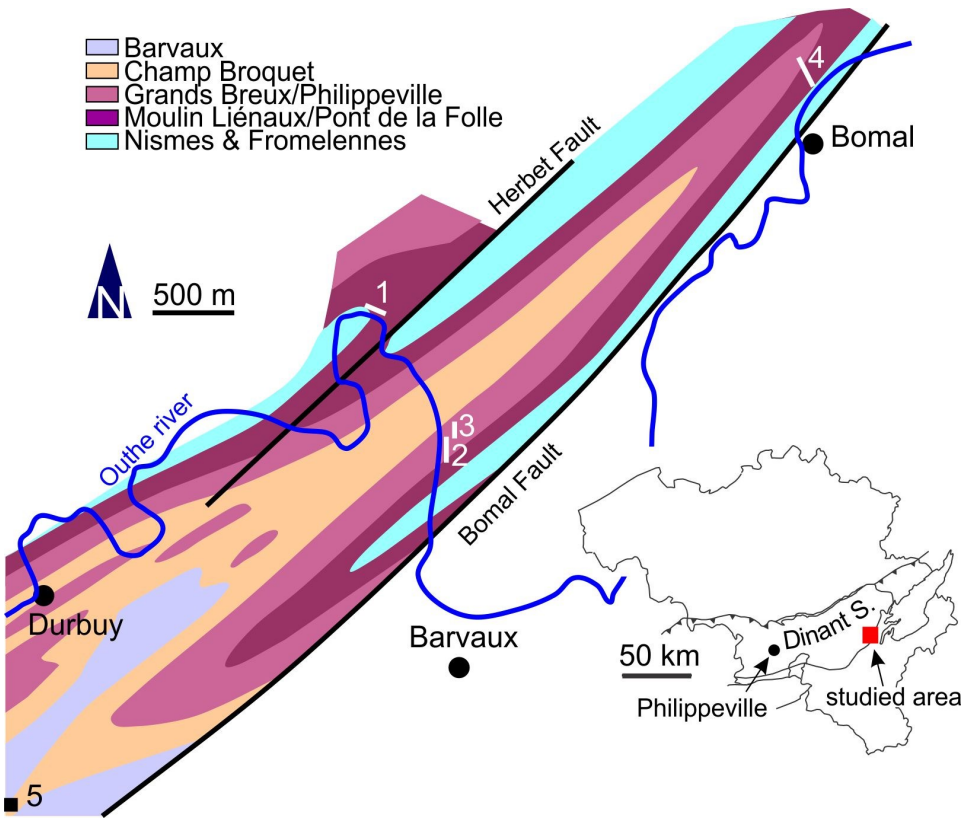

Figure 2. Schematic geological map of the Durbuy–Bomal area, with studied sections (1: Rocher Glawan; 2 & 3: Roche Plissée; 4: Ravin d'Herbet; 5: Rome). Modified after Coen (1974).

	IGN map	latitude	longitude	References
Rocher Glawan (Durbuy)	55/1	50°22'05" N	5°29'07" E	Point 13 (de Magnée, 1932); point 5 (Coen, 1974, fig. 6)
Roche Plissée (Durbuy)	55/1	50°21'43" N	5°29'27" E	Point 9 (de Magnée, 1932); point 3 (Coen, 1974, fig. 6)
Ravin d'Herbet (Durbuy)	49/5	50°22'50" N	5°31'17" E	Point 1 (Coen, 1974, fig. 6)
Rome mound (Durbuy)	55/1	50°20'29" N	5°27'10" E	Point 28 (de Magnée, 1932); point 13a (Coen, 1974, fig. 6; Dumon, 1982)

Table 1. Location of sections and references. IGN = National Geographical Institute.

Liège. The MS measurements were made using a KLY-3 Kappabridge device (see Da Silva & Boulvain, 2006). Three measurements were made on each sample weighed with a precision of 0.01g. Sampling interval varies, but is less than 1 m; 366 samples were analysed. Seven samples from the Roche Plissée section were selected for isotopic analyses of C and O performed at the Friedrich-Alexander-University of Erlangen-Nürnberg by Prof. M. Joachimski (see Joachimski, 1997 for analytical method). A microdrill was used to extract separately the matrix (micrite and microspar) and the cement (xenomorphic sparite).

3. Description of the sections

Along the Ourthe River, the **Rocher Glawan section** (Fig. 2; Fig. 3A; Fig. 4) makes the south limb of an anticline bordered to the south by the Herbet Fault. The axis of the anticline corresponds to more than 12 m of brownish shale with subsidiary calcareous beds or nodules. Fauna is rare, except for some brachiopods and numerous tabulate corals in the last bed before the next unit, which is a 14 m limestone unit, including an oligiste-rich bed 1 m above its base. The unit starts with a 2 m thick dark grey limestone rich in crinoids, brachiopods, tabulate corals and stromatoporoids, becoming more argillaceous and richer in fasciculate rugose corals upwards. On top of this bed, there is a 5 m unit made of grey massive limestone with disphyllids, lamellar tabulate corals and stromatoporoids. The section ends with 7 m of dark grey decimetre to metre-thick limestone beds with sparse corals and crinoids, alternating with shale.

The **Roche Plissée ("down") section** (Fig. 2; Fig. 4), also located along the Ourthe river, crops out in the southern flank of a syncline situated between the Herbet and Bomal Faults. It starts with dark brown shale, just below a first decimetre-thick bed of limestone, rich in brachiopods. The section continues with 25 m of alternating decimetre to metre-thick beds of dark grey crinoid and brachiopod-rich limestone, nodular limestone and shale. This unit grades upwards to 14 m of decimetre-thick dark grey argillaceous limestone with crinoids, brachiopods and a few solitary rugose corals. The last 4 m of this unit include three metre-thick lenses of light grey massive limestone with brachiopods, gastropods and corals. Finally, the section ends with 4 m of massive light grey limestone. Another section (**Roche Plissée "top"**; Fig. 2; Fig. 4), located above the former along the crest of the valley, was sampled to investigate possible lateral variations of the light grey massive limestone. It starts with 6 m of alternating metre-thick nodular dark grey limestone and decimetre to metre-thick light grey limestone. This unit grades upwards to 2 m of crinoids and brachiopod-rich limestone and ends with several metres of light grey massive limestone with crinoids and rugose and tabulate corals.

The **Ravin d'Herbet section** (Fig. 2; Fig. 3B; Fig. 4) corresponds to the southern flank of a syncline, between the Herbet and Bomal Faults. It was sampled along a thick dolomitic lens forming a headland (Rocher du Calvaire, Fig. 3B) and along a small valley joining the Herbet village and the Bomal station. The section starts with brownish shale. A 1.7 m hiatus separates the shale from 2 m of dark grey argillaceous limestone, the base of which is very rich in crinoids and becomes richer upwards in rugose corals and lamellar tabulate corals and stromatoporoids; a thin oligiste level was observed as in Rocher Glawan. The rugose corals of this first unit are represented by *Disphyllum hilli, D. grabaui* and *Macgeea rozkowskae* which are well known at the base of the Moulin Liénaux Formation as mentioned by Coen-Aubert (2009). The next unit is a 48 m thick dolomite lens. Only some rare corals or stromatoporoids escape the dolomitization process (see Fig. 7A). A 10 m thick hiatus separates the dolomitic lens from the second part of the section located along the Ravin d'Herbet itself and starting with 5 m of brown nodular shale followed by 9 m of alternating dark grey limestone, nodular limestone and shale with crinoids and brachiopods. This unit passes upwards to 4 m of dark grey limestone and 6 m of dark grey nodular limestone with crinoids and brachiopods. A 13 m thick hiatus separates this unit from the last one consisting of 4 m of light grey limestone with corals and brachiopods, followed by 4.5 m of dark limestone and 5 m of light grey, bedded limestone grading upwards to more massive limestone.

The 35 m high **Rome buildup** (Fig. 2; Fig. 5), located near the top of an SW plunging anticline, between the Herbet and Bomal Faults, is itself folded with its core being partially detached from the flank deposits. Several small SW-NE trending faults with an NW dipping intersected the buildup after the folding. The oldest mound facies, located in the lower central part of the quarry, is a red limestone with grey fibrous cement-filled stromatactis and scattered ossicles of crinoids. Locally, metre-sized lenses of dark bedded bioclastic limestone occur. After an argillaceous seam ("terrasse"), this 6 m thick red unit passes upwards to 18 m of a pink or grey limestone with decimetric massive rugose corals, branching and lamellar tabulate corals, scattered crinoids, brachiopods and lamellar stromatoporoids. This massive unit grades laterally to metre-thick lenses of pink limestone embedded in dark bioclastic argillaceous limestone. After a second argillaceous seam, the pink unit is topped by a red limestone with decimetric massive rugose corals, branching and lamellar tabulate corals, crinoids and smaller bioclasts, similarly passing laterally to flat lenses of red limestone surrounded by bioclastic flank deposits. The top of the mound corresponds to alternating dark grey limestone and shale with crinoids and rugose corals grading upwards to grey shale with brachiopods. A few colonies of *Frechastraea limitata* and *Potyphyllum ananas* have been identified in this quarry. According to Coen-Aubert (2016), these two species of rugose corals are common in the Petit-Mont Member, on the southeastern border of the Dinant Synclinorium.

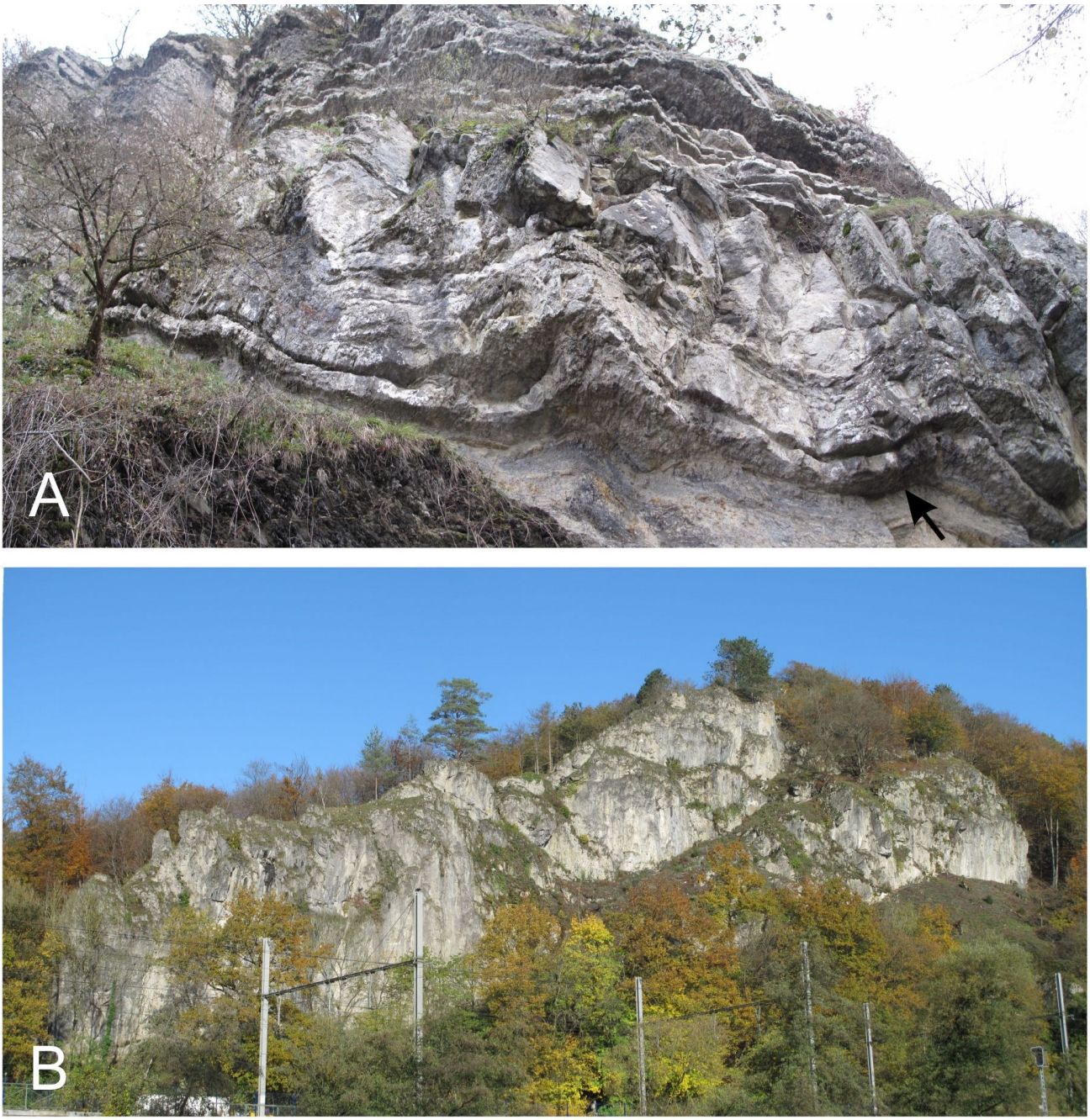

Figure 3. A: base of the Pont de la Folle Formation (arrowed) at the Rocher Glawan, along the Ourthe River. B: the dolomitic Brayelles Member in Bomal.

4. Lithostratigraphy

The stratigraphic relations of the different sections were already established by Coen (1974). However, the current formation names (Boulvain et al., 1999) were not used then and it seems necessary to propose up-to-date lithostratigraphic attributions (Fig. 6) (see Boulvain et al., 1999 for a historical overview).

The Rocher Glawan section is relatively easy to interpret with the shale unit corresponding to the Nismes Formation and the limestone unit to the Fontaine Samart Member of the Pont de la Folle Formation. The grey massive limestone is, therefore, an equivalent of the "Sainte-Anne Marble" of the authors (see for example Dumoulin & Marion, 1997b; Dumoulin, 2001 and Pas et al., 2015 for a description of this unit), but poorer in calcite-cemented fenestrae.

The stratigraphic interpretation of the Roche Plissée section is slightly more difficult than that of the previous one. The argillaceous dark limestone and shale could either be attributed to the base of the Philippeville Formation or the base of the Grands Breux Formation. The massive character of the upper grey unit resembles however that of the Lion Member and this macroscopic observation is supported by the occurrence of microbial limestone which has never been recorded in the Philippeville Formation (cf. Cornet, 1978; Boulvain et al., 1994), but is currently observed in the Frasnian mounds.

In the Ravin d'Herbet, the basal shale unit corresponds to the Nismes Formation whereas the 48 m thick dolomitic unit is attributed to the Brayelles Member of the Pont de la Folle Formation (see Dumoulin & Marion, 1997b; Dumoulin, 2001 for a description of the Brayelles Member). The upper nodular shale unit (Ermitage or Machenées Member) is observed in the upper part of the section. The end of the Ravin d'Herbet section corresponds to the Grand Breux Formation. This attribution is based on the characteristics of the alternating black argillaceous

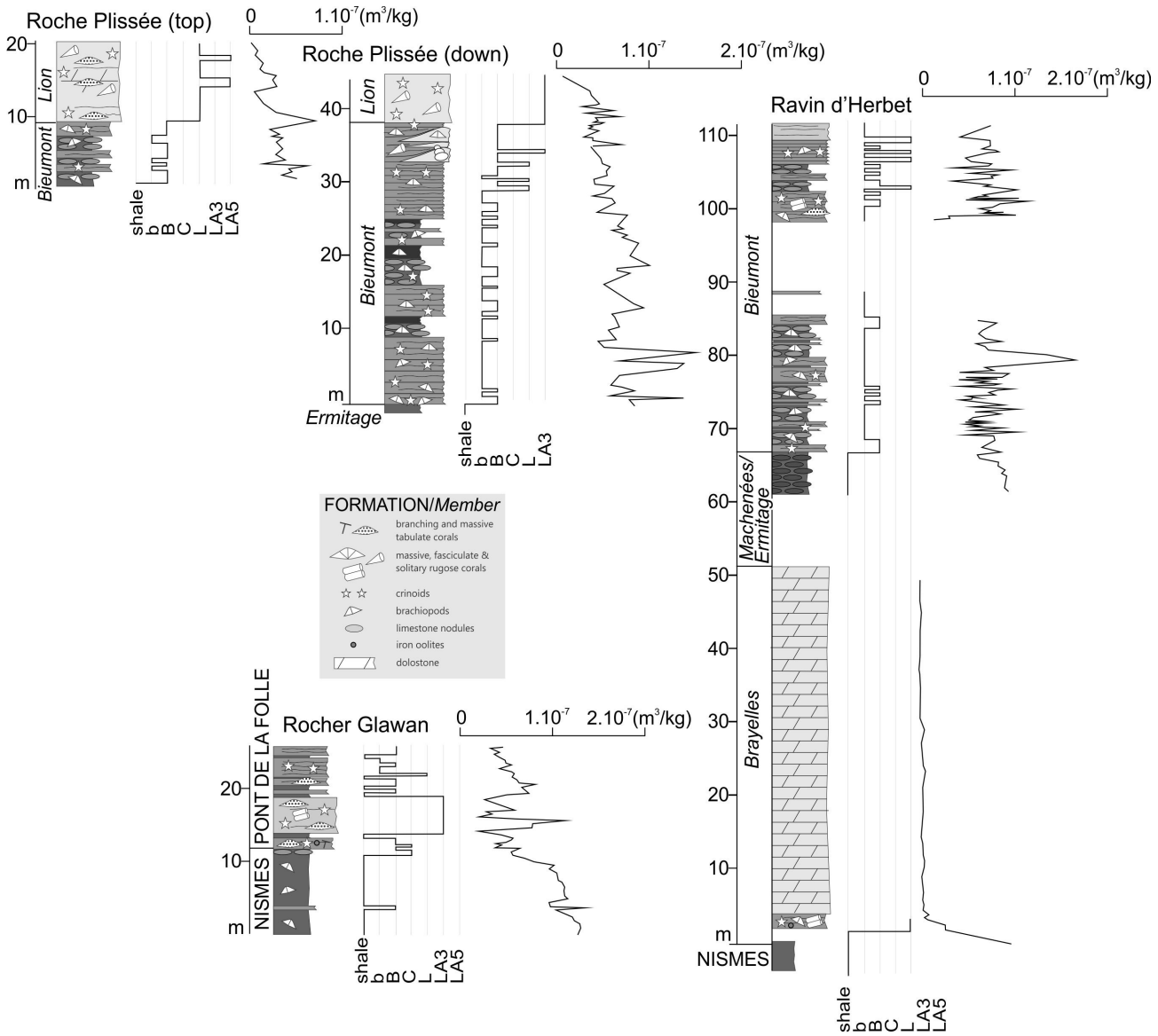

Figure 4. Logs of sections, with lithostratigraphy, microfacies and magnetic susceptibility.

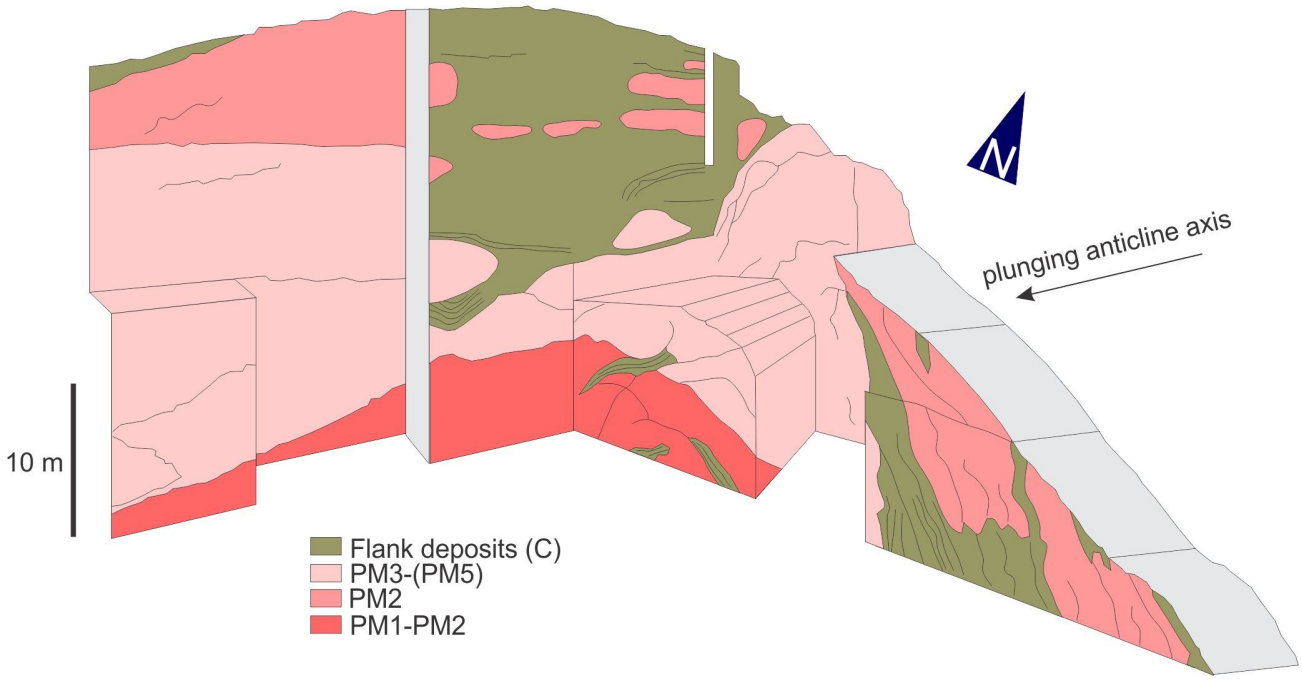

Figure 5. 3-D sketch of the Rome buildup with main facies (see Section 5).

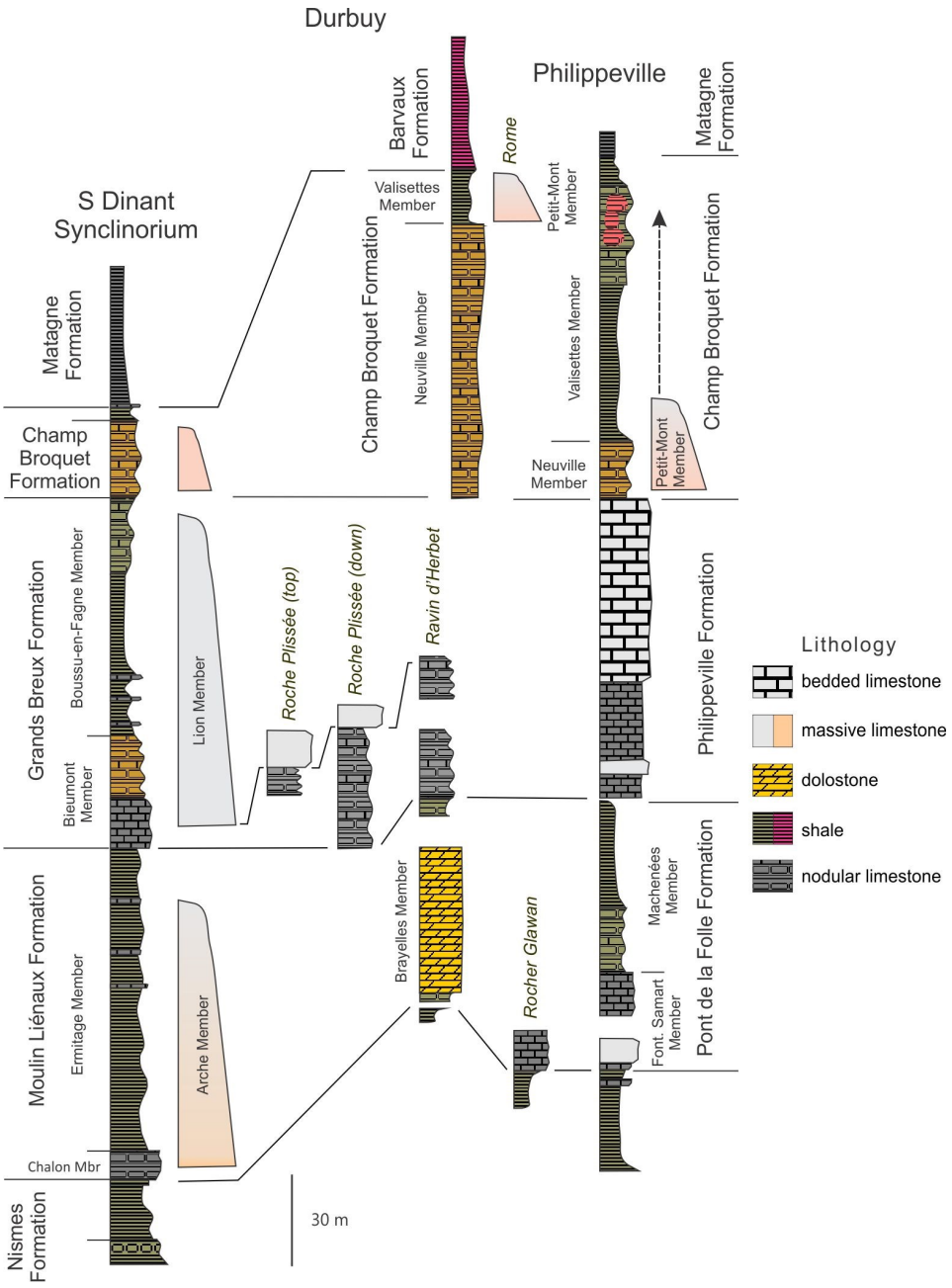

Figure 6. Correlation of studied sections with the Frasnian lithostratigraphic scheme (modified after Boulvain et al., 1999).

limestone and shale which correspond to the typical lithology of the Bieumont Member (Boulvain et al., 1999).

5. Microfacies

For a long time now, microfacies are widely used for standardizing petrographic descriptions of limestones (Wilson, 1975). In reefal carbonates, their use is even more useful by facilitating the identification of primary depositional geometries of homogeneous sedimentary units in complex buildups ("architecture" of reefs).

The Dunham (1962) textural classification for carbonates, expanded by Embry & Klovan (1971), is used throughout this paper. As several units surveyed in the Durbuy–Bomal area correspond obviously to well-known Frasnian reef mound carbonates, the corresponding microfacies, formerly proposed by Boulvain (2001, 2007) for the southern border of the Dinant Synclinorium and the Philippeville area, will be used herein. More precisely, reef mound microfacies include PM1-3 corresponding to the Petit-Mont Member and also LA3 and LA5 for the Lion Member. Flank and off-mound microfacies consist of microbioclastic (b), bioclastic (B), crinoidal (C) or lithoclastic (L) limestones (Boulvain, 2007). The observed microfacies are described hereunder, from the most distal to the most proximal for each model.

5.1. Reef mound microfacies

These microfacies are observed in rather massive, decimetre to metre-thick light grey, pink or red limestone beds.

Red wackestones and mudstones with stromatactis (PM1). The main characteristic of this microfacies is the occurrence of centimetric to decimetric stromatactis cemented by radiaxial calcite together with smaller irregular or stromatactoid fenestrae filled up with granular sparite (cf. Neuweiler et al., 2001). Microsparitic matrix is abundant. The main fossils are spicular networks and ostracods. Bryozoans, brachiopods, receptaculitids, trilobites and crinoids are sporadic. Occurrence: Rome buildup.

Red to pink wackestones and packstones with stromatactis, crinoids, corals (PM2). In addition to stromatactis, stromatactoid fenestrae are locally abundant. Fossils are more abundant than in PM1 and consist of crinoids, sponge spicules, ostracods,

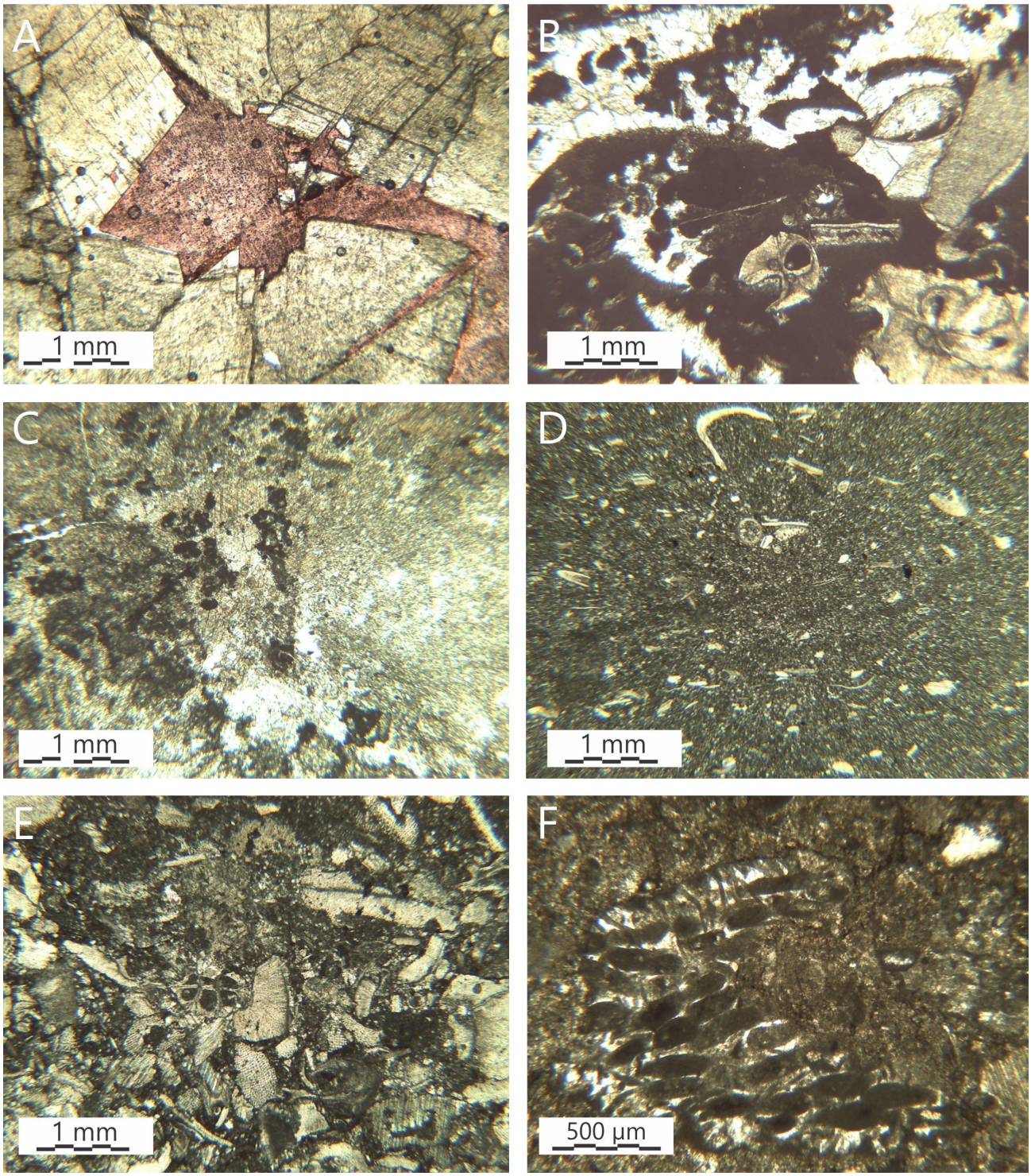

Figure 7. Examples of microfacies in thin section. A: saddle shape dolomite crystals and iron calcite (pink-coloured by alizarine), BOM15.7. B: wackestone with stromatactoid fenestrae, *Senceliaepora*, crinoids and brachiopod (PM2), RoM1. C: bafflestone with *Renalcis* (LA5), RPS500. D: microbioclastic mudstone-wackestone (b), GLA122b. E: bioclastic packstone with bryozoans, crinoids and brachiopods (B), GLA129. F: lithoclastic/peloidic packstone with *Paralitanaia* (L), BOM86. Natural light.

fenestellid bryozoans, gastropods, branching tabulate corals (*Thamnopora*, *Senceliaepora*) and solitary rugose corals (Fig. 7B). Occurrence: Rome buildup.

Pink to grey wackestones to grainstones with corals, crinoids, brachiopods, stromatactis and stromatactoid fenestrae (PM3). This microfacies includes all fossils observed in PM2 with additionally massive and fasciculate rugose corals as well as lamellar tabulate corals. The major difference with PM2 is the presence of 0.1–1 mm dark grey microbial peloids and different types of fossils coatings by *Girvanella* and/or *Sphaerocodium*. Some *Renalcis* bushes are observed and complete the assemblage. Locally, bioclasts and peloids are concentrated in millimetric to centimetric grainstone levels scattered in packstones or wackestones. These levels may pass laterally to centimetre-thick swarms of stromatactoid fenestrae. Occurrence: Rome buildup.

Pink to grey bafflestones with thrombolites and *Renalcis* (PM5). This microfacies is observed as pluridecimetric irregular lenses into PM3. Thrombolitic microbial structures (with a micritic clotted fabric sensu Aitken, 1967) are associated with

well-developed *Renalcis* bushes. Occurrence: Rome buildup.

Grey wackestones and floatstones with corals and stromatoporoids (LA3). The main fossils are lamellar tabulate corals and stromatoporoids, solitary and fasciculate rugose corals, brachiopods, crinoids, bryozoans, gastropods, and ostracods. Peloids and *Sphaerocodium* coatings are present. The matrix is micritic to microsparitic. Elongated millimetric to decimetric fenestrae (cemented "keystone vugs") are frequent below lamellar fossils: their base is covered with microsparitic internal sediment. Occurrence: Roche Plissée, Rocher Glawan.

Grey microbial bindstones, bafflestones, packstones and grainstones (LA5). This microfacies shows stromatolithic or thrombolithic microbial structures, often recrystallized, together with other cyanobacteria such as *Sphaerocodium, Girvanella, Renalcis* and unidentified dasycladales. Some stromatoporoids, brachiopods, bryozoans and corals may occur. Coatings are well developed and peloids are abundant. Matrix is microspar or recrystallized pseudospar (Fig. 7C). Occurrence: Roche Plissée (top).

5.2. Flank and off-mound microfacies

These microfacies are observed in well-bedded, centimetre to decimetre-thick, locally argillaceous or nodular, grey to dark grey limestone beds.

Dark grey microbioclastic mudstones, wackestones and packstones (b). The main fossils are small (<100 µm) broken fragments of crinoids, trilobites, ostracods, brachiopods, bryozoans and gastropods. Occasionally, some brachiopods are preserved. Bioturbation is locally well developed and consists of horizontal burrows 0.5–2.5 mm in diameter. Matrix is a slightly argillaceous microsparite, with pressure-solution seams and locally, tiny irregular peloids (<50 µm) (Fig. 7D). Occurrence: all sections excluding the Rome buildup.

Bioclastic wackestones, packstones and grainstones (B). This microfacies includes bigger (>0.3 mm) fossils than (b). Main fossils are crinoids with subordinate brachiopods, ostracods, bryozoans, trilobites and fragments of corals and stromatoporoids. Locally, lithoclasts are observed together with *Girvanella* and *Sphaerocodium* coatings fragments and calcispheres. Deformative bioturbation is present (Fig. 7E). Occurrence: all sections excluding the Rome buildup.

Rudstones with crinoids (C). Well-preserved crinoids dominate this microfacies. Other well-preserved fossils include bryozoans, ostracods, brachiopods, branching or lamellar tabulate corals, fasciculate or solitary rugose corals and lamellar stromatoporoids. Matrix is microsparitic and may be locally relatively argillaceous or replaced by granular sparitic calcite. Occurrence: Rocher Glawan and Rome sections.

Lithoclastic packstones and grainstones (L). Lithoclasts or peloids (millimetre-sized) are the main components of this microfacies. They are locally mixed with crinoids, brachiopods fragments, dendroid stromatoporoids, ostracods, calcispheres, paleosiphonocladales and rare dasycladales (*Paralitanaia*). Erosive structures are common together with deformative bioturbation (Fig. 7F). Occurrence: Ravin d'Herbet and La Roche Plissée sections.

6. Magnetic susceptibility

Broadly, changes in magnetic susceptibility (MS) in sedimentary successions are tentatively attributed to sea-level variations (Ellwood et al., 1999). Unfortunately, MS is a convolved signal and may reflect other processes than the often implicitly inferred depositional conditions. Diagenesis, remagnetization and low-grade metamorphism can potentially obscure the original, depositional MS signal (McCabe & Elmore, 1989; Zegers et al., 2003). However, a comparison of MS trends with palaeoenvironmental indicators (facies) and with detrital input proxies (Zr, Th, Ti, Al) allowed Da Silva et al. (2013) to assess the persistence of depositional trends in the Devonian rocks of Belgium. So, the major influence of sea level on the MS signal should be related to the strong link between MS and detrital components, assuming that the detrital input is generally controlled by eustasy or climate. In this way, a lowering of sea level (regression) increases the proportion of exposed continental area as well as the erosion and leads to higher MS values whereas a rising sea level (transgression) decreases MS (Crick et al., 2001). Climatic variations influence MS through changes in rainfall (high rainfall increases erosion and MS), glacial–interglacial periods (glacial periods are related to glacier erosion and marine regression and both effects increase MS) and pedogenesis (formation of magnetic minerals in soils; Tite & Linington, 1975).

The MS curves are plotted versus the logs and microfacies curves (Fig. 4) for the Roche Plissée, Rocher Glawan and Ravin d'Herbet sections. Tables 2 & 3 give the main results together with Figure 8 which shows the means and standard deviations for each microfacies.

	Mean	Standard deviation	Median	Number of samples
shale	92.61	24.23	94.0	33
b	69.36	26.01	69.0	100
B	59.70	34.66	59.5	74
C	53.67	6.81	56.0	3
L	44.50	25.50	48.5	16
LA3	46.13	23.40	41.0	24
LA5	16.58	10.09	15.5	12
dolomite	-0.29	1.47	0.0	24

Table 2. MS results ($x10^{-9}$ m^3/kg) for the Roche Plissée, Rocher Glawan and Ravin d'Herbet sections.

	Mean	Standard deviation	Median	Number of samples
PM1	10.00	5.66	10.0	2
PM2	11.11	7.64	7.5	33
PM3	8.93	5.85	8.0	45

Table 3. MS results ($x10^{-9}$ m^3/kg) for the Rome buildup.

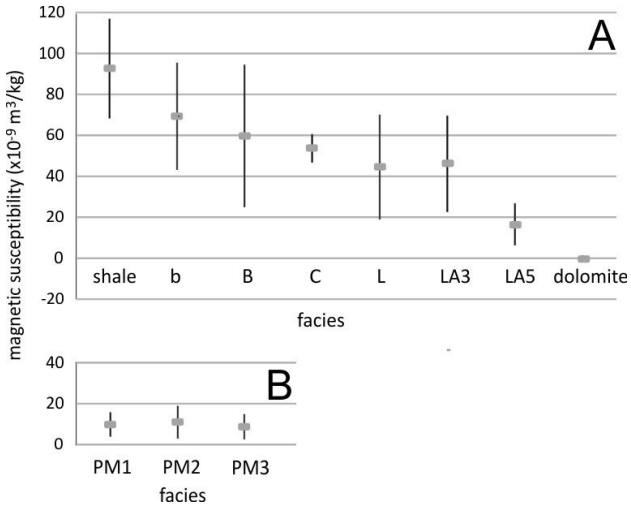

Figure 8. Plot of MS versus microfacies (mean and standard deviation) for the Roche Plissée, Rocher Glawan and Ravin d'Herbet sections (A) and Rome buildup (B). Name of microfacies: see Section 5.

7. Diagenesis

Dolomite is pervasive in the first part of the Bomal section (Fig. 7A), but it is observed in all the other sections, both as minute rhombohedral crystals scattered in the matrix and larger xenomorphic saddle shape crystals replacing calcite in veins and fenestrae (cf. Folk & Assereto, 1974). The first one is generally related to pressure-solution seams (Wanless, 1979). Cathodoluminescence observation of thin sections from Rome and La Roche Plissée shows that the diagenetic sequence is as follows: (1) radiaxial calcite, (2) automorphic non-luminescent calcite, succeeded by (3) a bright orange luminescent fringe, (4) granular xenomorphic calcite with a dull orange luminescence (Fig. 9), (5) iron-bearing saddle dolomite.

Samples were taken from La Roche Plissée "top" section (Lion Member) for $\delta^{13}C$ and $\delta^{18}O$ stable isotope analysis. Matrix and cement from fenestrae were separated. The results are plotted in Figure 10.

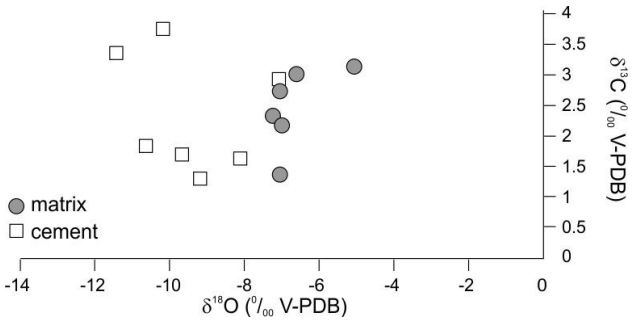

Figure 10. Plot of $\delta^{13}C$ versus $\delta^{18}O$ for samples from the La Roche Plissée section.

8. Discussion

8.1. Depositional environments

The PM1-5 microfacies are frequently observed in the Petit-Mont Member reef mounds whose architecture is currently well known (e.g. Delhaye, 1913; Lecompte, 1956; Dumon, 1957; Tsien, 1984; Boulvain, 2001). Data obtained from the Rome buildup will be compared below with other Petit-Mont Member examples.

Unfortunately, the base of the Rome reef mound, ideally corresponding to the first occurrence of red massive limestone over grey argillaceous or nodular limestone, is not visible in the quarry. The oldest facies is PM1, characterised by the presence of stromatactis, red hematitic pigment and very low organic diversity. Stromatactis are now widely interpreted as cavities left by degrading sponges in gel-like sediment (Bourque & Boulvain, 1993). This interpretation accounts for the striking horizontal flat bottom of all stromatactis, due to the slow deposition of fine-grained internal sediment in the primary cavity (Wallace, 1987). The red pigment is attributed to the local development of microaerophilic iron bacteria (Boulvain et al., 2001) which, together with the sponge-dominated low diversity community, fine-grained texture and lack of algae, suggests a relatively deep marine environment below the photic and storm wave zones. The PM2 microfacies recorded a noticeable increase in diversity, but the lack of algae and the fine-grained character of the sediment, together with the presence of some delicate branching forms, still point to a deep and quiet

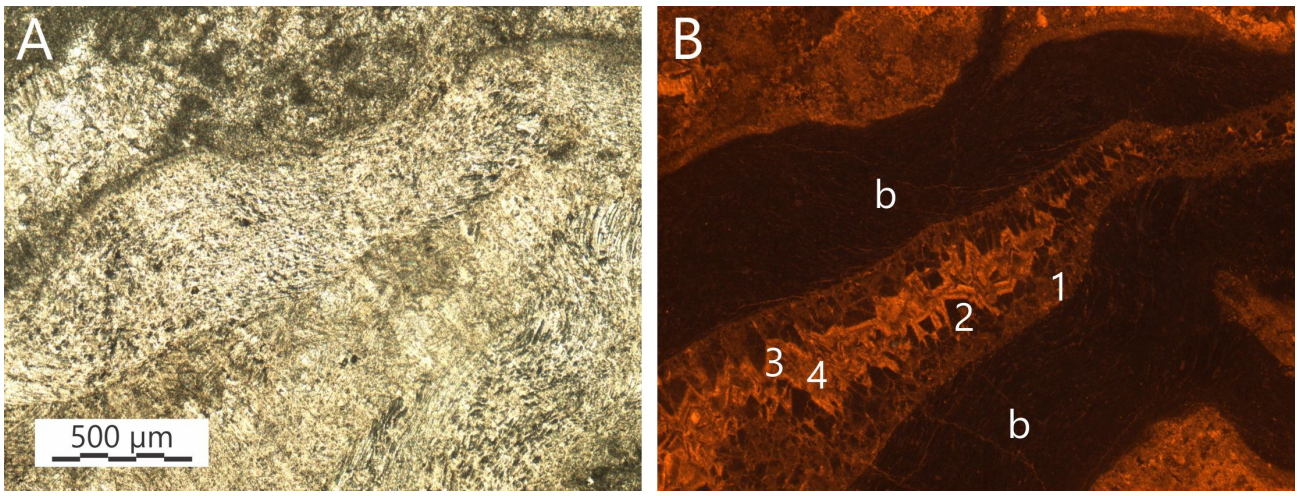

Figure 9. A: internal cementation in a brachiopod shell; natural light. B: centripetal cementation in cathodoluminescence: successively: heavily recrystallized radiaxial calcite (1), scalenohedral non-luminescent calcite (2), bright orange luminescent fringe (3), and (4) dull orange xenomorphic calcite. The brachiopod shell (b) is made of non-luminescent calcite. Sample RPS 499.

environment. The less homogeneous character of this microfacies could explain the replacement of the large stromatactis cavities by networks of small stromatactoid fenestrae in the zones richest in grains (Boulvain, 2001; Neuweiler et al., 2001). In the third mound microfacies PM3, the presence of cyanobacteria and small local lenses of thrombolites (PM5) suggests deposition in the photic zone. Occasional beds of coarser material were due to temporary increases in turbulence near the storm wave zone. Moreover, storms likely caused some gravity flows visible on the flanks of the mound. These mound microfacies are surrounded by argillaceous or nodular limestone with crinoids (microfacies C). This is classically observed around a lot of Petit-Mont Member mounds in Belgium and other Paleozoic examples in the world (e.g. Burchette, 1981; Krause & Meyer, 2004).

The size of the Rome buildup is hard to determine accurately, due to partial outcropping. However, this size should be slightly lesser than its Philippeville equivalents which have a thickness of 60 m for a diameter of 150 m (Boulvain, 2007). The 3-D architecture of the Rome buildup can be reconstructed from the study of microfacies distribution (Fig. 5). The lower part of the mound is characterised by alternating PM1 and PM2 (Fig. 11A). The middle part is dominated by microfacies PM3 (with lenses of PM5, Fig. 11B & C) and the upper part by a recurrence of PM2 (Fig. 11D). It is worth noting that this upper part also corresponds to a dramatic reduction in the mound diameter, with a retrogradation of the carbonate facies PM2 and the onset of well-developed flank deposits (Fig. 5). Local metric lenses of PM2 were still present, embedded within the flank microfacies. This evolution was already emphasized by Lecompte (1956) working on the Petit-Mont mounds from the Philippeville area and interpreted as a consequence of a sea-level rise during the final development stage of the buildups. Conversely, the PM1-PM2-PM3 transition should be the result of a bathymetric decrease together with a progressive maturation of organic communities (Olszewski, 2016; Purkis et al., 2016). As already stated by de Magnée (1932), no well-developed core with grey algal or microbial facies (PM4 and PM5, Boulvain, 2001) is observed in the Rome buildup. However, small thrombolitic lenses are present, like in the Beauchâteau mound (Boulvain & Coen-Aubert, 1992). Actually, this does not mean that core facies did not develop because observations from the Philippeville area have shown that in many cases, this grey limestone was totally removed during the operational phase of the quarry.

The LA3 and LA5 microfacies are commonly observed in most middle Frasnian buildups along the southern border of the Dinant Synclinorium (Lion and Arche Members). LA3 resembles PM3 forming the bulk of the Petit-Mont Member Rome mound, in all but the colour. Notably, the organic community of LA3 is similar to PM3. LA3 is characterised by a relatively diversified community, dominated by reef builders and by the common occurrence of cyanobacteria, suggesting deposition close to the photic zone. The present work shows that this microfacies is also observed near the base of the Pont de la Folle Formation (Fontaine Samart Member) in the Rocher Glawan section. This particular occurrence of the Fontaine Samart Member built up over a striking bioclasts-bryozoans sole and is remarkable for well-developed multiple encrustations of lamellar tabulate corals, stromatoporoids, bryozoans and algae. The origin of the keystone fenestral structures observed below these fossils is not fully understood but is most likely related to the presence of lamellar corals or stromatoporoids, limiting vertically the collapse of the roof of the cavities left by the degradation of sponges (Wallace, 1987; Boulvain, 2001). LA5 is characterised by widely developed microbial structures in isolated or connected colonies and coatings of skeletal elements.

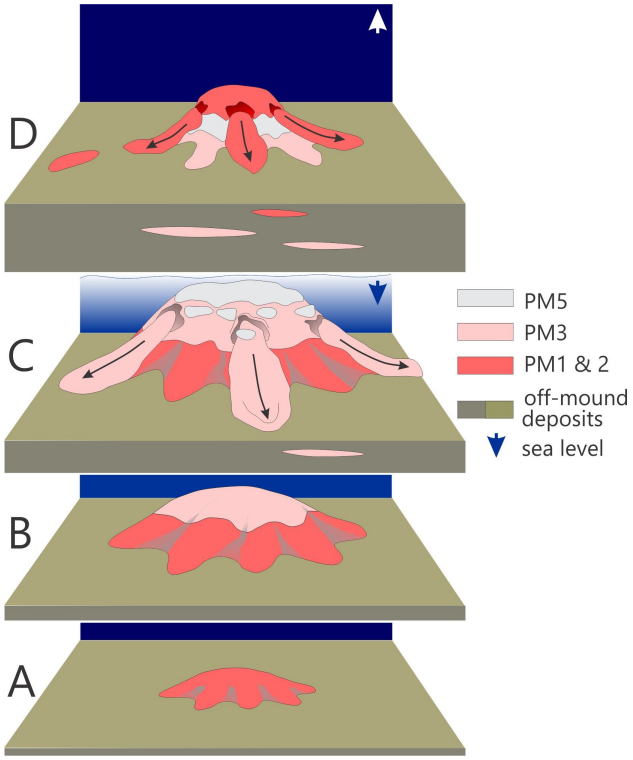

Figure 11. Model of development of Petit-Mont Member reef mounds. A: initiation of mound development below the photic and wave action zones. B: diversification stage. C: progradation and entering in the storm wave zone, development of photic communities and reworking of material by gravity flows. D: retrogradation and drowning of the mound.

For the interpretation, much emphasis is placed on the presence of green algae in this microfacies, together with prevalent grainy textures indicating a development in the photic and fair-weather wave zones.

Middle Frasnian Arche and Lion mounds along the southern border of the Dinant Synclinorium are known to be relatively large buildups, reaching 150 m in thickness and nearly 1 km in diameter (Boulvain, 2007). The few Lion Member beds cropping out in the La Roche Plissée sections reach 9 m only, corresponding to the very lower part of the mound. Therefore, due to limited outcropping, no attempt to reconstruct the 3-D geometry of these mounds was made. The dolomitized Brayelles Member in the Ravin d'Herbet is almost 66 m thick, which is exactly comparable to its type locality (cf. Dumoulin & Marion, 1997b).

In the Roche Plissée ("down") section, below the base of the grey massive mound limestone, three metric lenses with similar LA3 facies were observed, probably corresponding to a starting stage of the mound. As a matter of fact, several studies suggested that a lot of reef mounds are the result of coalescing isolated patch reefs (e.g. Zampetti et al., 2004). It is worth noting that the first mound microfacies developing over bedded limestone or bedded argillaceous limestone from the Bieumont Member are LA3 or LA5. The first case is usual in the classical Lion outcrops (Frasnes, La Boverie, Boulvain et al., 2004; Humain, Moulin Bayot, Boulvain et al., 2005). Conversely, the LA5 microfacies abruptly topping the Bieumont Member (La Roche Plissée "top") was never observed up to now. It is suggested that during the progressive lateral expansion of the mound, lenses of microbial limestone (LA5) directly prograded over the surrounding sediments.

Microbioclastic (b) and bioclastic (B) microfacies are

ubiquitous in flank and off-mound settings. Dominated by open-marine organisms, they represent background sedimentation on an external carbonate platform or ramp. Crinoidal rudstones (C) are mainly observed on mound flanks where slopes ensure an acceleration of food-carrying bottom currents (Macurda & Meyer, 1977). This type of habitat is the rule in a lot of Paleozoic mounds (Burchette, 1981). Lithoclastic packstones and grainstones (L) are more remarkable: according to their position and characteristics, they may result from the input of eroded material exported directly from the buildups by gravity flows (Stoakes, 1980) or from the reworking and sorting of already deposited material by storm waves (Humblet & Boulvain, 2001). The occurrence of microfacies (L) in the Roche Plissée and Ravin d'Herbet sections only, associated with a Lion buildup, and the presence of green algae suggest that the first explanation should be preferred: the lithoclastic material was reworked from shallow parts of the buildups and deposited as grain flows in off-reef environments. A similar microfacies was observed in the close vicinity of the Nord quarry (Frasnes) by Boulvain & Coen-Aubert (1998). This observation suggests that the Lion buildup from which the reworked material originated reached its full development, like in Frasnes or Jemelle (Boulvain et al., 2004, 2005).

8.2. Magnetic susceptibility

The MS values obtained from all the sections range from -4 to 164 x 10^{-9} m^3/kg (mean: 47 x 10^{-9} m^3/kg, standard deviation: 35 x 10^{-9} m^3/kg). This is consistent with lots of other Upper Paleozoic platform limestones (see Bertola et al., 2013 for a review). A comparison between the MS and microfacies curves exhibits similar trends (Fig. 4), suggesting that the MS signal is primary. Moreover, the MS values regularly decrease from the off-mound microfacies (shale) to the reef mound microfacies (LA3-5, PM1-3) (Table 2; Fig. 8A). The same pattern was already recorded for Frasnian Belgian and Canadian carbonate buildups (Da Silva et al., 2009). This was interpreted by the former authors as the consequence of local water agitation in the shallower parts of a buildup, preventing the detrital particles from settling down and to the higher sedimentation rate that dilutes the magnetic minerals. Why MS values from the Rome buildup are clearly lower than from the other sections, despite the presence of an iron pigment, is not clear yet (Fig. 8B).

8.3. Diagenesis

Samples from the matrix and cemented cavities are clearly separated in Figure 10. The mean $\delta^{18}O$ (6.7‰ vs Pee Dee Belemnite, PDB) of the matrix is consistent with published values for Frasnian marine carbonates (Veizer et al., 1986; -5.5 to -7.5‰ vs PDB) while the mean $\delta^{13}C$ (2.45‰ vs PDB) is slightly higher than the proposed values for the same Frasnian carbonates (Veizer et al., 1986; -1 to 2‰ vs PDB). For what concerns the cement, the mean $\delta^{18}O$ values (-9.5‰ vs PDB) are systematically lower than the published values for Frasnian marine cements (i.e. Kerans et al., 1986: -4.3‰ vs PDB; Carpenter & Lohmann, 1989: -5‰ vs PDB), while the mean $\delta^{13}C$ values (2.4‰ vs PDB) are consistent with these published values (i.e. Kerans et al., 1986: 1.9‰ vs PDB; Carpenter & Lohmann, 1989: 2‰ vs PDB). The cement stable isotopes values are much close to the "stage 4" (granular xenomorphic sparite) obtained from the Petit-Mont Member mounds in the Philippeville area (Boulvain, 2001). This stage was interpreted as a burial cement.

The diagenetic sequence observed in La Roche Plissée and Rome sections is exactly similar to that illustrated by Boulvain (2001) for the Petit-Mont buildups in the Philippeville area. It is also identical to diagenetic sequences of other Paleozoic carbonate mounds and banks (Miller, 1986; Lees & Miller, 1995): cementation in the marine phreatic zone preliminary to drowning, then the development of a meteoric lens at the time of a marine regression, with dysoxic facies in the distal zones of the aquifer and, finally burial cementation and dolomitization during the Variscan tectonism.

8.4. Palaeogeography

The aim here is, by integrating the lateral organization of palaeoenvironments, to propose a palaeogeographic interpretation of the Frasnian platform in the eastern part of the Dinant Synclinorium and to compare this model with its southern border and with the Philippeville area.

The Rome buildup is very similar to its equivalents in the Philippeville area and may be attributed to the Les Wayons mound type (cf. Boulvain, 2001), characterised by high synsedimentary relief, well-developed flanks, vertical and lateral microfacies zonation, presence of microfacies PM3 and well-marked retrograding final stage with a reoccurrence of PM1 and PM2. As the mound type has been shown to be related to bathymetry (Fig. 12), it is suggested that the Durbuy and Philippeville areas underwent the same environmental conditions throughout the end of Frasnian.

Concerning the other sections (Fig. 6), two main areas are easily distinguished from the field data, microfacies, lithostratigraphic and structural interpretations (Bellière, 1954; Barchy & Marion, 2008): the Durbuy area with the Rocher Glawan section differs from all the other successions by the occurrence of the Fontaine Samart Member of the Pont de la Folle Formation typical of the western part of the Philippeville area (Dumoulin et al., 1998) (Fig. 1). The Roche Plissée and Ravin d'Herbet sections, on the opposite, are dominated by reef mound facies (Lion and Brayelles Members) commonly observed in the eastern part of the Philippeville area, the Beaumont area and the southern border of the Dinant Synclinorium (Dumoulin et al., 1998). In this model, the two successions correspond respectively to a middle platform with bedded limestone and an external platform with reef mounds. In the Philippeville area, these two domains are separated by thrust faults (one of these faults was observed in the Merlemont quarry, cf. Boulvain et al., 1994). In the Durbuy–Bomal area, the Herbet Fault may have played a similar role. Additionally, it is interesting to mention that in the Ravin d'Herbet section, the Bieumont Member of the Grand Breux Formation succeeds the Brayelles and Machenées Members of the Pont de la Folle Formation.

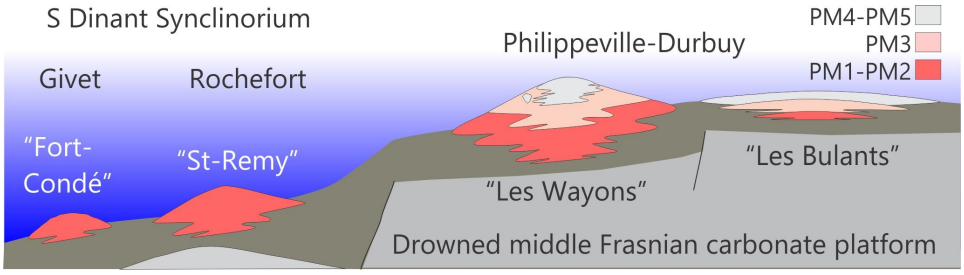

Figure 12. Bathymetric control on the Petit-Mont Member mounds. This sketch corresponds to the period just before the late Frasnian sea-level rise.

In all the sections, facies are dominated by dark argillaceous limestone with an open-marine fauna (crinoids, brachiopods, bryozoans, trilobites…) locally interrupted by the development of mounds (Lion, Brayelles Members) or fore-reef coral carpets (Fontaine Samart Member). Nowhere the conditions for shallow restricted sedimentation were met. This allows us to exclude the hypothesis of a "lagoon" in the Bomal area (Coen, 1974). Moreover, the so-called "dolomitized barrier" in the same area is more likely related to dolomitized reef mounds, as in the Philippeville area (the Philippeville Formation in the Merlemont quarries; Boulvain et al., 1994) and the Beaumont area (Dumoulin & Marion, 1997b).

9. Conclusions

A multidisciplinary study (field work, petrography, magnetic susceptibility, O and C stable isotopes) of Frasnian formations in the Durbuy–Bomal area led to an improved palaeogeographical interpretation of reef mound development in the eastern part of the Dinant Synclinorium. Four sections were studied and sampled: Rocher Glawan, Roche Plissée, Ravin d'Herbet and Rome. The first section is located north of the Herbet fault whereas the other three are situated between the Herbet and Bomal Faults.

Lithostratigraphically, the Nismes Formation and the Fontaine Samart Member were identified in the Rocher Glawan; the Ermitage, Bieumont and Lion Members in the Roche Plissée; the Nismes Formation, Brayelles, Machenées/Ermitage and Bieumont Members in the Ravin d'Herbet and finally, the Petit-Mont Member in the Rome buildup. This underlines the complexity of the eastern Dinant Synclinorium where tectonic units typical from the southern border of the Dinant Synclinorium and from the Philippeville area are juxtaposed or interfingered. More particularly, this is due in the Durbuy–Bomal area to the succession of narrow folds often complicated by longitudinal faults.

Petrographically, massive mound limestone includes microfacies typical for the Petit-Mont and Lion Members, characterised by micritic textures and fossil associations respectively dominated by sponges (PM1), sponges, crinoids and corals (PM2), corals, crinoids, stromatoporoids and cyanobacteria (PM3 and LA3) and microbes (PM5 and LA5). Flank and off-mound microfacies consist of microbioclastic, bioclastic, crinoidal or lithoclastic bedded limestones.

MS values are rather low and consistent with other Upper Paleozoic platform limestones. They appear to be related to the depositional environment and are regularly decreasing from the off-mound microfacies to the reef mound microfacies, mainly due to the influence of increasing water agitation and sedimentation rate.

The diagenetic sequence observed in the mound microfacies is similar to that identified in the Petit-Mont buildups from the Philippeville area: cementation in the marine phreatic zone preliminary to drowning, then the development of a meteoric lens at the time of a marine regression, with dysoxic facies in the distal zones of the aquifer and, finally burial cementation and dolomitization during the Variscan tectonism.

Palaeogeographically, the Rome buildup developed in the same palaeoenvironments as its Philippeville equivalents, as well as the Fontaine Samart Member in the Rocher Glawan section. All the other sections show reef mound facies (Lion and Brayelles Members) commonly observed in the Beaumont area and the southern border of the Dinant Synclinorium. No evidence of lagoonal facies was observed in the area.

Acknowledgements

The authors are most grateful to J-M. Marion for sharing unpublished geological maps and notes and to Z. Belka and an anonymous reviewer for interesting suggestions that greatly improved this paper.

Author contribution

Field work, petrography and preliminary interpretations: N. Demaude and F. Toussaint. Field work, petrography, final interpretation and synthesis: F. Boulvain and M. Coen-Aubert. Article writing: F. Boulvain.

Data availability

All samples and thin sections are stored at the University of Liège, Laboratoire de Pétrologie sédimentaire.

References

Aitken, J.D., 1967. Classification and environmental significance of cryptalgal limestones and dolomites, with illustrations from the Cambrian and Ordovician of Southwestern Alberta. Journal of Sedimentary Petrology, 37, 1163–1178. https://doi.org/10.1306/74D7185C-2B21-11D7-8648000102C1865D

Barchy, L. & Marion, J-M., 2008. Carte géologique de Wallonie : Maffe – Grandhan 54/3-4. 1/25 000. Ministère de la Région wallonne, Direction générale des ressources naturelles et de l'environnement, Namur, avec une notice explicative de 64 p.

Bellière, J., 1954. Quelques particularités de la tectonique de la région comprise entre Hamoir et Durbuy. Annales de la Société géologique de Belgique, 77, B167–B177.

Bertola, C., Boulvain, F., Da Silva, A.-C. & Poty, E., 2013. Sedimentology and magnetic susceptibility of Mississippian (Tournaisian) carbonate sections in Belgium. Bulletin of Geosciences, 88, 69–82. https://doi.org/10.3140/bull.geosci.1339

Boulvain, F., 2001. Facies architecture and diagenesis of Belgian Late Frasnian carbonate mounds (Petit-Mont Member). Sedimentary Geology, 145, 269–294. https://doi.org/10.1016/S0037-0738(01)00152-X

Boulvain, F., 2007. Frasnian carbonate mounds from Belgium: sedimentology and palaeoceanography. In Álvaro, J.J., Aretz, M., Boulvain, F., Munnecke, A., Vachard, D. & Vennin, E. (eds), Palaeozoic Reefs and Bioaccumulations: Climatic and Evolutionary Controls. Geological Society, London, Special Publications, 275, 125–142. https://doi.org/10.1144/GSL.SP.2007.275.01.09

Boulvain, F. & Coen-Aubert, M., 1992. La carrière de marbre rouge de Beauchâteau : aperçu paléontologique, stratigraphique et sédimentologique. Annales de la Société géologique de Belgique, 115, 19–22.

Boulvain, F. & Coen-Aubert, M., 1998. Le monticule frasnien de la carrière du Nord à Frasnes (Belgique) : sédimentologie, stratigraphie séquentielle et coraux. Geological Survey of Belgium, Professional Papers, 285, 47 p.

Boulvain F., Coen-Aubert, M., Dumoulin, V. & Marion, J-M., 1994. La Formation de Philippeville à Merlemont : contexte structural, comparaison avec le stratotype et paléoenvironnements. Service géologique de Belgique, Professional Papers, 269, 30 p.

Boulvain, F., Bultynck, P., Coen, M., Coen-Aubert, M., Lacroix, D., Laloux, M., Casier, J-G., Dejonghe, L., Dumoulin, V., Ghysel, P., Godefroid, J., Helsen, S., Mouravieff, N., Sartenaer, P., Tourneur, F. & Vanguestaine, M., 1999. Les Formations du Frasnien de la Belgique. Memoirs of the Geological Survey of Belgium, 44, 125 p.

Boulvain, F., De Ridder, C., Mamet, B., Préat, A. & Gillan, D., 2001. Iron microbial communities in Belgian Frasnian carbonate mounds. Facies, 44, 47–60. https://doi.org/10.1007/BF02668166

Boulvain, F., Cornet, P., Da Silva, A-C., Delaite, G., Demany, B., Humblet, M., Renard, M. & Coen-Aubert, M., 2004. Reconstructing atoll-like mounds from the Frasnian of Belgium. Facies, 50, 313–326. https://doi.org/10.1007/s10347-004-0014-9

Boulvain, F., Demany, B. & Coen-Aubert, M., 2005. Frasnian carbonate buildups of southern Belgium: the Arche and Lion members interpreted as atolls. Geologica Belgica, 8, 69–91.

Bourque, P.A. & Boulvain, F., 1993. A model for the origin and petrogenesis of the red stromatactis limestone of Paleozoic carbonate mounds. Journal of Sedimentary Petrology, 63, 607–619. https://doi.org/10.1306/D4267B8B-2B26-11D7-8648000102C1865D

Burchette, T.P., 1981. European Devonian reefs: a review of current concepts and models. In Toomey, D.F. (ed.), European Fossil Reef Models. Society for Economic Paleontologists and Mineralogists, Special Publications, 30, 85–142. https://doi.org/10.2110/scn.83.02.0000

Carpenter, S.J. & Lohmann, K.C., 1989. $\delta^{18}O$ and $\delta^{13}C$ variations in Late Devonian marine cements from the Golden Spike and Nevis reefs, Alberta, Canada. Journal of Sedimentary Petrology, 59, 792–814. https://doi.org/10.1306/212F9075-2B24-11D7-8648000102C1865D

Coen, M., 1973. Faciès, conodontes et stratigraphie du Frasnien de l'Est de la Belgique pour servir à une révision de l'étage. Annales de la Société géologique de Belgique, 95, 239–253.

Coen, M., 1974. Le Frasnien de la bordure orientale du Bassin de Dinant. Annales de la Société géologique de Belgique, 97, 67–103.

Coen-Aubert, M., 2009. Fasciculate rugose corals across the Early-Middle Frasnian boundary in Belgium. Bulletin de l'Institut royal des Sciences naturelles de Belgique, Sciences de la Terre, 79, 55–86.

Coen-Aubert, M., 2015. Revision of the genus *Frechastraea* Scrutton, 1968 (Rugosa) in the Upper Frasnian of Belgium. Geologica Belgica, 18, 109–125.

Coen-Aubert, M., 2016. *Potyphyllum*, a new phillipsastreid genus of rugose corals in the Upper Frasnian of Belgium with precisions about the age of the Petit-Mont Member. Geologica Belgica, 19, 165–175. https://doi.org/10.20341/gb.2015.016

Cornet, P., 1978. Le biostrome "F2h" de la tranchée du chemin de fer de Neuville (Bassin de Dinant - Belgique). Annales de la Société géologique de Belgique, 100, 31–40.

Crick, R.E., Ellwood, B.B., Hladil, J., El Hassani, A., Hrouda, F. & Chlupác, I., 2001. Magnetostratigraphy susceptibility of the Pridolian–Lochkovian (Silurian–Devonian) GSSP (Klonk, Czech Republic) and a coeval sequence in Anti-Atlas Morocco. Palaeogeography, Palaeoclimatology, Palaeoecology, 167, 73–100. https://doi.org/10.1016/S0031-0182(00)00233-9

Da Silva, A.-C. & Boulvain, F., 2006. Upper Devonian carbonate platform correlations and sea level variations recorded in magnetic susceptibility. Palaeogeography, Palaeoclimatology, Palaeoecology, 240, 373–388. https://doi.org/10.1016/j.palaeo.2006.02.012

Da Silva, A.-C., Potma, K., Weissenberger, J.A., Whalen, M.T., Humblet, M., Mabille, C. & Boulvain, F., 2009. Magnetic susceptibility evolution and sedimentary environments on carbonate platform sediments and atolls, comparison of the Frasnian from Belgium and Alberta, Canada. Sedimentary Geology, 214, 3–18. https://doi.org/10.1016/j.sedgeo.2008.01.010

Da Silva, A.-C., De Vleeschouwer, D., Boulvain, F., Claeys, P., Fagel, N., Humblet, M., Mabille, C., Michel, J., Sardar Abadi, M., Pas, D. & Dekkers, M.J., 2013. Magnetic susceptibility as a high-resolution correlation tool and as a climatic proxy in Paleozoic rocks - Merits and pitfalls: Examples from the Devonian in Belgium. Marine and Petroleum Geology 46, 173–189. https://doi.org/10.1016/j.marpetgeo.2013.06.012

Delhaye, F. 1913. Etude de la formation des récifs de calcaire rouge à *Acervularia* et *Hypothyris cuboïdes*. Annales de la Société géologique de Belgique, 40, B469–B481.

de Magnée, I, 1930. La stratigraphie du Frasnien dans la région de Durbuy - Grand Han. Annales de la Société géologique de Belgique, 54, B116–B124.

de Magnée, I, 1932. Compte rendu de la session extraordinaire organisée à Barvaux-sur-Ourthe du 16 au 19 septembre 1932 par la Société géologique de Belgique. Annales de la Société géologique de Belgique, 55, B251–B313.

Dumon, P., 1957. Note sur les marbres rouges en Belgique. Publication de l'Association des Ingénieurs de la Faculté polytechnique de Mons, 3, 1–41.

Dumon, P., 1982. Aperçu historique de l'activité marbrière en Wallonie. Annales des Mines de Belgique, 1982/11, 945–1008.

Dumoulin, V., 2001. Carte géologique de Wallonie : Grandrieu – Beaumont 52/5-6. 1/25 000. Ministère de la Région wallonne, Direction générale des ressources naturelles et de l'environnement, Namur, avec une notice explicative de 70 p.

Dumoulin, V. & Marion, J-M., 1997a. Carte géologique de Wallonie : Sautour – Surice 58/1-2. 1/25 000. Ministère de la Région wallonne, Direction générale des ressources naturelles et de l'environnement, Namur, avec une notice explicative de 70 p.

Dumoulin, V. & Marion, J-M., 1997b. Carte géologique de Wallonie : Silenrieux – Walcourt 52/7-8. 1/25 000. Ministère de la Région wallonne, Direction générale des ressources naturelles et de l'environnement, Namur, avec une notice explicative de 75 p.

Dumoulin, V., Marion, J.-M., Boulvain, F., Coen-Aubert, M. & Coen, M., 1998. Nouvelles données lithostratigraphiques sur le Frasnien de l'Anticlinorium de Philippeville. Annales de la Société géologique du Nord, 6 (2e série), 79–85.

Dunham, R.J., 1962. Classification of carbonate rocks according to depositional texture. American Association of Petroleum Geologists Memoirs, 1, 108–121.

Ellwood, B.B., Crick, R.E. & El Hassani, A., 1999. The Magneto-Susceptibility Event and Cyclostratigraphy (MSEC) method used in geological correlation of Devonian rocks from Anti-Atlas Morocco. American Association of Petroleum Geologists Bulletin, 83, 1119–1134. https://doi.org/10.1306/E4FD2E8D-1732-11D7-8645000102C1865D

Embry, A.F. & Klovan, J.E., 1971. A Late Devonian reef tract on northeastern Banks Island, N.W.T. Bulletin of Canadian Petroleum Geology, 19, 730–781. https://doi.org/10.35767/gscpgbull.19.4.730

Folk, R.L. & Assereto, R., 1974. Giant aragonite rays and baroque white dolomite in tepee-fillings, Triassic of Lombardy, Italy (abstract). American Association of Petroleum Geologists. Abstracts with program, Annual Meeting, 34–35.

Fourmarier, P., 1900. Etude du Givetien et de la partie inférieure du Frasnien au bord oriental du Bassin de Dinant. Annales de la Société géologique de Belgique, 27, Mémoires, 49–110.

Fourmarier, P., 1931. La faille de la Jastrée (Barvaux). Annales de la Société géologique de Belgique, 54, B327–B331.

Fourmarier, P., 1954. La tectonique. In Fourmarier, P. (ed.), Prodrome d'une Description géologique de la Belgique. Société géologique de Belgique, Liège, 609–744.

Humblet, M. & Boulvain, F. 2001. Sedimentology of the Bieumont Member: influence of the Lion Member carbonate mounds (Frasnian, Belgium) on their sedimentary environment. Geologica Belgica, 3, 97–118. https://doi.org/10.20341/gb.2014.026

Joachimski, M., 1997. Comparison of organic and inorganic carbon isotope patterns across the Frasnian-Famennian boundary. Palaeogeography, Palaeoclimatology, Palaeoecology, 132, 133–145. https://doi.org/10.1016/S0031-0182(97)00051-5

Kerans, C., Hurley, N.F. & Playford, P.E., 1986. Marine diagenesis in Devonian reef complexes of the Canning Basin, Western Australia. In Schroeder, J.H. & Purser, B.H. (eds), Reef Diagenesis. Springer, Berlin, 357–380.

Krause, R.A. Jr & Meyer, D.L., 2004. Sequence stratigraphy and depositional dynamics of carbonate buildups and associated facies from the Lower Mississippian Fort Payne Formation of southern Kentucky, U.S.A. Journal of Sedimentary Research, 74, 831–844. https://doi.org/10.1306/042504740831

Lecompte, M., 1956. Quelques précisions sur le phénomène récifal dans le Dévonien de l'Ardenne et sur le rythme sédimentaire dans lequel il s'intègre. Bulletin de l'Institut royal des Sciences naturelles de Belgique, 32/21, 39 p.

Lees, A. & Miller, J., 1995. Waulsortian banks. In Monty, C.L.V., Bosence, D.W.J., Bridges, P.H. & Pratt, B.R. (eds), Carbonate Mud -Mounds: Their Origin and Evolution. International Association of Sedimentologists, Special Publication, 23, 191–271.

Macurda, D.B.Jr. & Meyer, D.L., 1977. Crinoids of West Indian coral reefs. In Frost, S.H., Weiss, M.P. & Saunders, J.B. (eds), Reefs and Related Carbonates—Ecology and Sedimentology. American Association of Petroleum Geologists, Studies in Geology, 4, 195–207. https://doi.org/10.1306/St4393C18

McCabe, C. & Elmore, R.D., 1989. The occurrence and origin of Late Paleozoic remagnetization in the sedimentary rocks of North America. Reviews of Geophysics, 27, 471−494. https://doi.org/10.1029/RG027i004p00471

Miller, J., 1986. Facies relationships and diagenesis in Waulsortian mudmounds from the Lower Carboniferous of Ireland and N. England. In Schroeder, J.H. & Purser, B.H. (eds), Reef Diagenesis. Springer, Berlin, 311–335.

Neuweiler, F., Bourque, P-A. & Boulvain, F., 2001. Why is stromatactis so rare in Mesozoic carbonate mud mounds? Terra Nova, 13, 338–346. https://doi.org/10.1046/j.1365-3121.2001.00367.x

Olszewski, T.D., 2016. Biological self-organization: implications for sedimentary rocks with examples from shallow marine settings. SEPM Society for Sedimentary Geology, Special Publication, 106, 40–52. https://doi.org/10.2110/sepmsp.106.03

Pas, D., Da Silva, A. C., Devleeschouwer, X., De Vleeschouwer, D., Labaye, C., Cornet, P., Michel, J. & Boulvain, F., 2015. Sedimentary development and magnetic susceptibility evolution of the Frasnian in Western Belgium (Dinant Synclinorium, La Thure section). In Da Silva, A-C., Whalen, M.T., Hladil, J., Chadimova, L., Chen, D., Spassov, S., Boulvain, F. & Devleeschouwer, X. (eds), Magnetic Susceptibility Application: A Window onto Ancient Environments and Climatic Variations. Geological Society, London, Special Publications, 414, 15–36. https://doi.org/10.1144/SP414.7

Purkis, S.J., Van de Koppel, J. & Burgess, P.M., 2016. Spatial self-organization in carbonate depositional environments. SEPM Society for Sedimentary Geology, Special Publication, 106, 53–66. https://doi.org/10.2110/sepmsp.106.02

Sacré, R., 1943. Contribution à l'étude de la tectonique de la bordure sud du bassin de Dinant entre Dourbes et Villers-le-Gambon. Annales de la Société géologique de Belgique, 66, B74–B84.

Stoakes, F.A. 1980. Nature and control of shale basin fill and its effect on reef growth and termination: Upper Devonian Duverney and Ireton Formations of Alberta, Canada. Bulletin of Canadian Petroleum Geology, 28, 345–410. https://doi.org/10.35767/gscpgbull.28.3.345

Tite, M.S. & Linington, R.E., 1975. Effect of climate on the magnetic susceptibility of soils. Nature, 256, 565–566. https://doi.org/10.1038/256565a0

Tsien, H.H., 1984. Récifs du Dévonien des Ardennes - Paléoécologie et structure. In Geister, J. & Herb, R. (eds), Géologie et Paléoécologie des Récifs. Institut géologique de l'Université de Berne, 7.1–7.30.

Veizer, J., Fritz, P. & Jones, B., 1986. Geochemistry of brachiopods: oxygen and carbon isotopic records of Paleozoic oceans. Geochimica et Cosmochimica Acta, 50, 1679–1696. https://doi.org/10.1016/0016-7037(86)90130-4

Wallace, M.W., 1987. The role of internal erosion and sedimentation in the formation of Stromatactis mudstones and associated lithologies. Journal of Sedimentary Petrology, 57, 695–700. https://doi.org/10.1306/212F8BDE-2B24-11D7-8648000102C1865D

Wanless, H.R., 1979. Limestone response to stress: pressure solution and dolomitization. Journal of Sedimentary Petrology, 49, 437–462. https://doi.org/10.1306/212F7766-2B24-11D7-8648000102C1865D

Wilson, J.L., 1975. Carbonate Facies in Geologic History. Springer, Berlin, 471 p. https://doi.org/10.1007/978-1-4612-6383-8

Zampetti, V., Schlager, W., van Konijnenburg, J.H. & Everts, A.J., 2004. Architecture and growth history of a Miocene carbonate platform from 3D seismic reflection data; Luconia province, offshore Sarawak, Malaysia. Marine and Petroleum Geology, 21, 517–534. https://doi.org/10.1016/j.marpetgeo.2004.01.006

Zegers, T.E., Dekkers, M.J. & Baily, S., 2003. Late Carboniferous to Permian remagnetization of Devonian limestones in the Ardennes: role of temperature, fluids and deformation. Journal of Geophysical Research, 108/B7, 2357. https://doi.org/10.1029/2002JB002213